JOURNAL OF SOLID STATE CHEMISTRY 135, 210–217 (1998)
ARTICLE NO. SC977623

Nickel–Iron Alloy/Magnetite Composites: Synthesis and Microstructure

J. C. Yamegni Noubeyo, T. Bouakham, G. Pourroy,[1] J. Werckmann, and G. Ehret

Institut de Physique et de Chimie des Matériaux de Strasbourg, Groupe des Matériaux Inorganiques, UMR 046 du CNRS, 23 Rue du Loess F-67037 Strasbourg Cedex, France

Received March 27, 1997; in revised form September 9, 1997; accepted September 12, 1997

We describe the procedure to obtain composites made of a nickel–iron alloy and magnetite. A KOH concentration of 14 mol/liter is required. Metal diffraction lines are broad, due to heterogeneous composition and bad crystallization. Balls of metal 0.1–0.2 μm wide stuck to magnetite octahedra are easily observed by SEM and TEM. Nickel hydroxide crystallizes for a nickel to iron ratio >0.33 in addition to metal and spinel. HRTEM shows metal and spinel grains covered by a thin layer of NiO crystals of 20 nm recovered by an amorphous phase 2–3 nm wide. This latter crystallizes in NiO under the electron beam. Crystallographical relationships occur between NiO and the spinel phase. Well-crystallized and hydroxide-free nickel–iron alloy/magnetite composites are obtained in all cases after annealing at 800°C in an argon atmosphere. © 1998 Academic Press

INTRODUCTION

Metal ceramic composites are widely studied for their mechanical or magnetic properties (1, 2). For instance, the combination of high thermal stability of ceramic oxides with the ductility of metals in order to increase the strength and the toughness of ceramics has attracted considerable attention in recent years (3). Magnetic properties of fine metallic particles embedded into an insulator matrix such as SiO_2 and Al_2O_3 have also given rise to numerous studies (4–7). Several synthetic methods have been used, including the reduction of small particles of oxides or high energy ball milling (4, 5, 8, 9).

A novel method for synthesizing metal–oxide composites is to use a disproportionation reaction leading to a metal on one side and to an oxide on the other. This idea has been recently developed in our laboratory by using Fe(II) disproportionation in a concentrated and boiling KOH medium (10). It leads to a α-Fe/Fe_3O_4 composite made up of small grains of 0.5–1.5 μm which do not oxidize below 100°C in air. This is surprising since powders of magnetite or metal of such a fine granulometry oxidize rapidly at room temperature. This disproportionation reaction has also been used to synthesize other composites. Indeed, as metallic iron reduces Co(II), it has been possible to obtain composites made up of iron–cobalt alloy and cobalt containing magnetite (11, 12). They are obtained in a narrow domain of KOH concentration, e.g., 11.5–13.5 mol/liter for Co/Fe = 0.33. This domain is shifted toward higher values when the cobalt concentration is decreased (13). For instance, [KOH] must be higher than 15 mol/liter for Co/Fe = 0. Composites having hysteresis curves characterized by high coercive fields of 2000–3000 Oe at room temperature can be easily obtained (14). Such high values were unknown for materials involving ferrites. Transmission electron microscopy has demonstrated that the metal is embedded in the spinel phase located near the edges and overlaid by a poorly crystallized layer or misshapen regions containing small spinel crystals and amorphous phases; i.e., the metal is never directly in contact with air (15).

The nickel-based system is not as well known. It has been shown that a 14 mol/liter KOH concentration and an annealing in vacuum at 800°C are required for obtaining a pure composite when Ni/Fe = 0.5 (16). This paper is devoted to nickel-based composites with Ni/Fe ratios between 0 and 0.5. The effects of KOH concentration on the composition and purity of the phases are described.

EXPERIMENTAL

Aqueous solutions of chlorides $FeCl_2 \cdot 4H_2O$ and $NiCl_2 \cdot 6H_2O$ were prepared at room temperature. Aqueous KOH solutions were refluxed in a stainless steel vessel equipped with a mechanical stirrer on a hot plate. The temperature was measured by means of a stainless steel thermometer placed in the center of the vessel. The metal chloride solution was added to the KOH by means of a peristaltic pump at a rate of 10 ml/min. During the following maturation time of 20 min, heating and stirring were maintained. The black precipitate formed was then filtered from the hot solution,

[1] To whom correspondence should be addressed.

0022-4596/98 $25.00

washed with boiling water and ethanol, and dried at 40°C in air. It was then annealed under argon at 800°C for 15 h.

Let us define $[KOH]_i$ as the concentration of potassium hydroxide before the addition of metal chloride solution and $[M]_i$ as the concentration of the metal ions (iron and nickel) before being added to KOH. The boiling temperature of potassium hydroxide increases when $[KOH]_i$ increases from 120°C for $[KOH]_i$ = 9mol/liter to 155°C for $[KOH]_i$ = 15 mol/liter. $[KOH]_i$ was varied from 7 to 15 mol/liter. Solutions of nickelous and ferrous chlorides with a total metal concentration of 1.5 mol/liter and $[Ni]_i/[Fe]_i$ ratio of 0, 0.1, 0.2, 0.33, and 0.5 were prepared. Volumes of KOH and chlorides are chosen to have $[KOH]_i/[KOH]_f = 1.3$.

The samples were analyzed by the Induced Coupled Plasma method at the Laboratoire Central d'Analyse de Vernaison CNRS in order to give the overall $[Ni]_f/[Fe]_f$ ratio in the final product. X-ray diffraction data were collected at room temperature by use of a D500 Siemens diffractometer equipped with a quartz monochromator ($CoK\alpha_1$ = 1.78897 Å). Observations of the morphology of the samples were performed with a JEOL scanning electron microscope. Thermogravimetric (TG) and differential thermal (DTA) analyses were carried out in platinum crucibles in air or in vacuum by using a Setaram 92 apparatus. The temperature was increased at a rate of 1 K/min. The variation in weight was calculated after subtracting the weight of the empty crucible. High-resolution transmission electron microscopy (HRTEM) and energy-dispersive X-ray spectroscopy (EDXS) were used to obtain microstructural information, determine individual grain compositions, and identify phases. To solve the problem of aggregation between the small magnetic particles and to avoid their loss in the pole piece of the microscope, the powders were ground and embedded in Epon 812, carefully mixed. Thin samples were obtained using an ultramicrotome equipped with a diamond knife. The 60–90 nm thick sections were collected on holey, carbon coated, 200 mesh copper grids and examined with a TOPCON 002B microscope operating at 200 kV (point to point resolution of 0.18 nm) and equipped with an ultrathin window KEVEX EDX spectrometer. For EDXS analysis, the standard spinel material $NiFe_2O_4$ was used to check the validity of the K factors and of the correction parameters used for the deconvolution computation. Fifteen spectra were collected from which the atomic ratio of Fe to Ni was found to be 2 ± 0.01. Thus, thickness and fluorescence have minor effects on the results. Because of the large absorption correction necessary for the low energy X-rays characteristic of oxygen, data from this element was not used for quantitative analysis. Nevertheless, the data were used for fast localization of oxide and metallic phases. Following calibration with the (111) and (220) spots of monocrystalline silicon, HRTEM was used to directly determine the lattice parameters.

RESULTS

1. *Procedure for Obtaining Ni–Fe Alloy/Spinel Composites*

X-ray diffraction patterns are presented in Fig. 1 for $[Ni]_i/[Fe]_i = 0.2$ and various $[KOH]_i$, and in Fig. 2 for

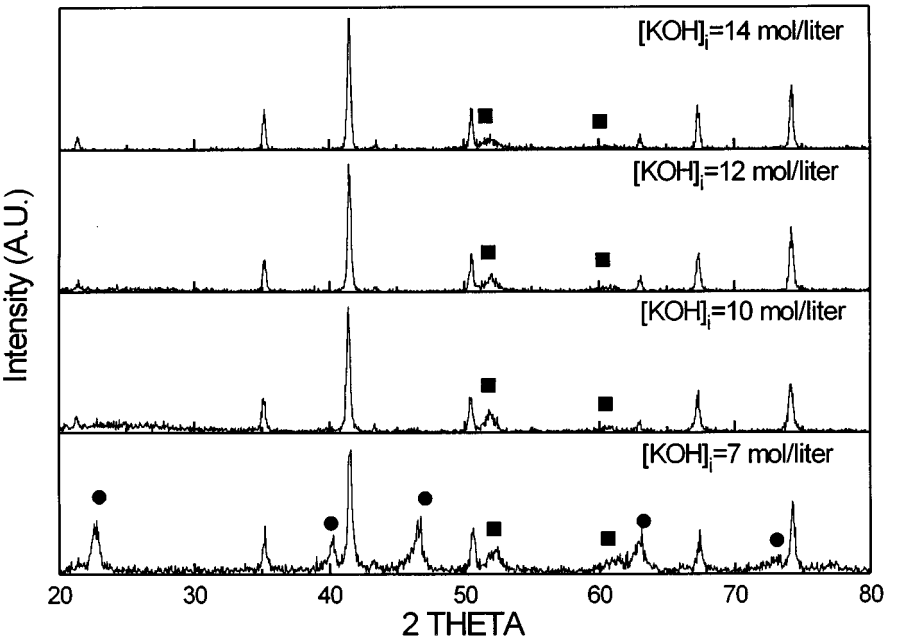

FIG. 1. X-ray diffraction patterns of composites with $[Ni]_i/[Fe]_i = 0.2$ and $[M]_i = 1.5$ mol/liter and $[KOH]_i/[KOH]_f = 1.3$. ■ and ● represent the metallic phase and hydroxide isomorphous to $Ni(OH)_2$ respectively. The other diffraction lines correspond to magnetite.

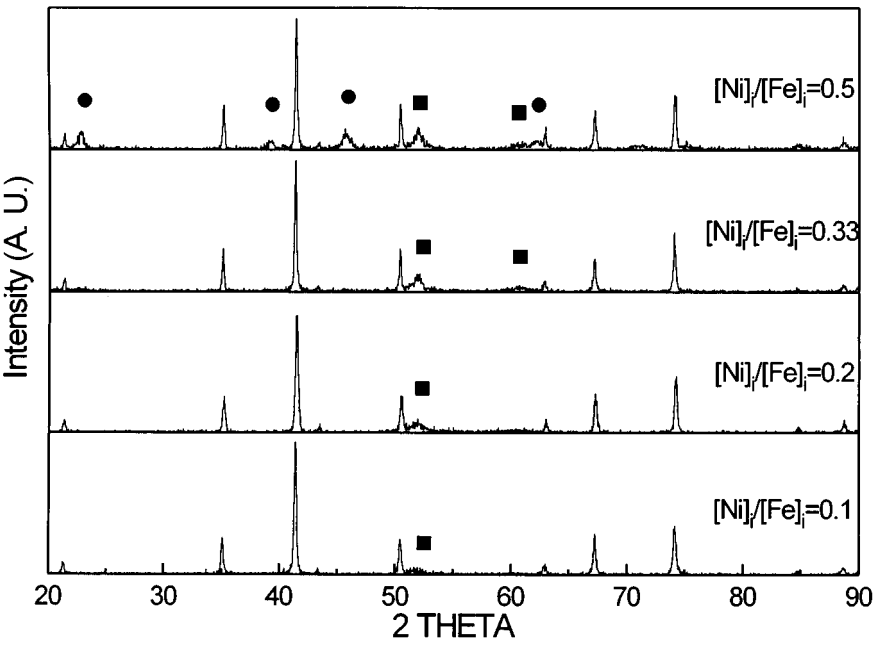

FIG. 2. X-ray diffraction patterns of composites with $[Ni]_i/[Fe]_i = 0.1$, 0.2, 0.33, and 0.5 and $[KOH]_i/[KOH]_f = 1.3$. ■ and ● represent the metallic phase and hydroxide isomorphous to $Ni(OH)_2$, respectively. The other diffraction lines correspond to magnetite.

$[KOH]_i = 14$ mol/liter and $[Ni]_i/[Fe]_i = 0.1$, 0.2, 0.33, and 0.5. A metallic phase of fcc structure and a spinel phase are crystallized in all cases. The lattice parameter of the spinel phase is found to be between 8.390 (4) and 8.408 (5) Å (Table 1), i.e. close to that of magnetite ($a = 8.392$ Å) and very far from that of nickel ferrite ($a = 8.339$ Å). The diffraction lines of the metal are so large that it is impossible to determine its lattice constant. For $[KOH]_i = 14$ mol/liter, the background is zero. It increases when $[KOH]_i$ decreases, showing that amorphous phases occur (Fig. 1). For $[KOH]_i$ below 10 mol/liter, hydroxide isomorphous of $Ni(OH)_2$ with $a = 3.01(2)$ Å and $c = 4.50(2)$ Å arises. Furthermore, the intensities of the metal diffraction lines increase when $[KOH]_i$ decreases. For $[Ni]_i/[Fe]_i = 0.5$, $Ni(OH)_2$ crystallizes in addition to the metal and the spinel phase. The global composition of the composites $[Ni]_f/[Fe]_f$ is equal to $[Ni]_i/[Fe]_i$, ruling out a loss of metallic ions in the filtrate. TG measurements performed in air show that a weight loss occurs below 150°C (Fig. 3). It increases when Ni/Fe increases, from 0.5% for Ni/Fe = 0.1 up to 4.7% for 0.33. TG cycles between 20 and 150°C show this loss to be reversible; thus it is probably due to adsorption of carbonates or water. Above 150°C, the composite oxidizes; therefore, a weight increase is observed in the TGA curve and two peaks in the DTA curve. However, it is difficult to assign these peaks, because they can be due to the oxidation of either metal and magnetite, or small and large grains.

The annealing at 800°C under argon improves the crystallization particularly for the metal (Fig. 4). The lattice constant of the spinel phase remains close to the magnetite

TABLE 1
Lattice Parameters of Spinel and Metal Phases in the Samples Prepared with $[KOH]_i = 14$ mol/liter, Before* and After an Annealing at 800°C in an Argon Atmosphere**

$[Ni]_i/[Fe]_i$	0.1	0.2	0.33	0.5
a_{spinel} (Å)*	8.393(3)	8.408(5)	8.403(3)	8.390(4)
a_{spinel} (Å)**	8.398(2)	8.401(3)	8.394(3)	8.370(2)
a_{metal} (Å)**	3.538(2)	3.545(1)	3.530(1)	3.526(1)
Fe% in the alloy**	13%	20%	8%	4%
Δm/m in air (%)**	4.3	6.2	6.9	6.8
Composition**	$(Fe^0_{0.13}Ni^0_{0.87})_{0.20}$ $[Fe_{2.89}Ni_{0.11}O_4]$	$(Fe^0_{0.2}Ni^0_{0.8})_{0.54}$ $[Fe_{2.84}Ni_{0.16}O_4]$	$(Fe^0_{0.08}Ni^0_{0.92})_{0.78}$ $[Fe_{2.78}Ni_{0.22}O_4]$	$(Fe^0_{0.02}Ni^0_{0.98})_{0.87}$ $[Fe_{2.55}Ni_{0.45}O_4]$

Note. Weight increase in air and chemical formula. The composition of the alloys is deduced from Ref. (17).

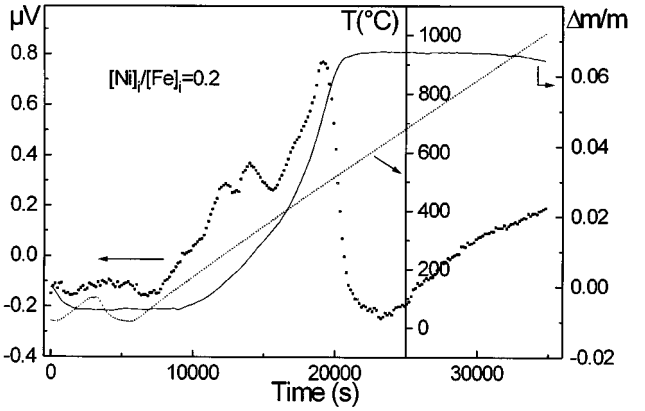

FIG. 3. TGA (—) and DTA (···) curves obtained under air for $[Ni]_i/[Fe]_i = 0.2$.

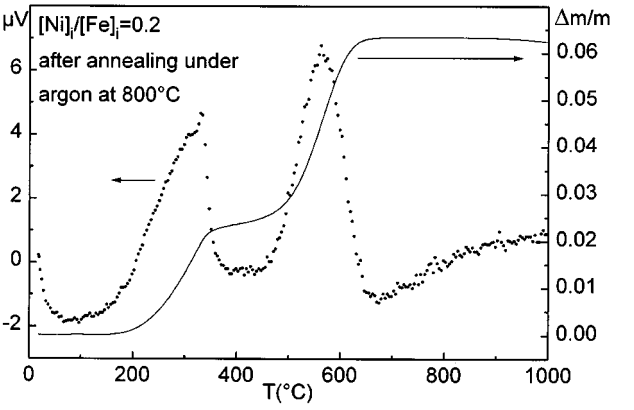

FIG. 5. TGA (—) and DTA (···) curves obtained under air for $[Ni]_i/[Fe]_i = 0.2$ after an annealing at 800°C under argon.

one after annealing for $[Ni]_i/[Fe]_i = 0.1$, 0.2, and 0.33. It decreases for $[Ni]_i/[Fe]_i = 0.5$, showing that the spinel phase of the precipitate transforms into a nickel containing magnetite (Table 1). No weight loss is observed by annealing in vacuum (Fig. 5). Therefore, the weight increase observed by TG measurements in air allows one to determine the chemical formula, taking into account the composition of the metal deduced from the lattice constants, and the ratio Ni to Fe in the composite (Table 1). The iron ratio in the metal decreases when $[Ni]_i/[Fe]_i$ increases from 0.2 to 0.5. Indeed, as the reduction of Ni(II) by Fe^0 is thermodynamically favored and as the global nickel ratio in the material increases, the metallic phase tends to enrich in nickel. However, it is not pure nickel, because the annealing time is too low to allow a complete redistribution of nickel and iron between both phases. Surprisingly, the sample with $[Ni]_i/[Fe]_i = 0.1$ is richer in nickel than expected from the last considerations. This is due to a low metal/spinel ratio because of a partial oxidation of metallic iron during the synthesis. Consequently, the quantity of nickel is enough to give a nickel rich alloy.

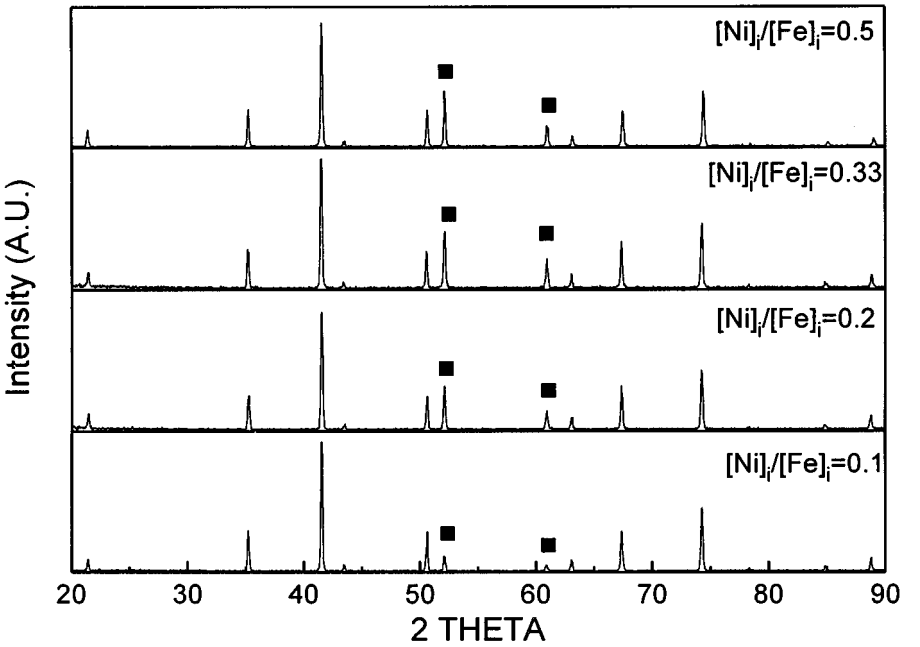

FIG. 4. X-ray diffraction patterns of composites annealed in an argon atmosphere at 800°C with $[Ni]_i/[Fe]_i = 0.1$, 0.2 0.33, and 0.5. $[KOH]_i = 14$ mol/liter, $[M]_i = 1.5$ mol/liter. ■ represents the metallic phase. The other diffraction lines correspond to magnetite.

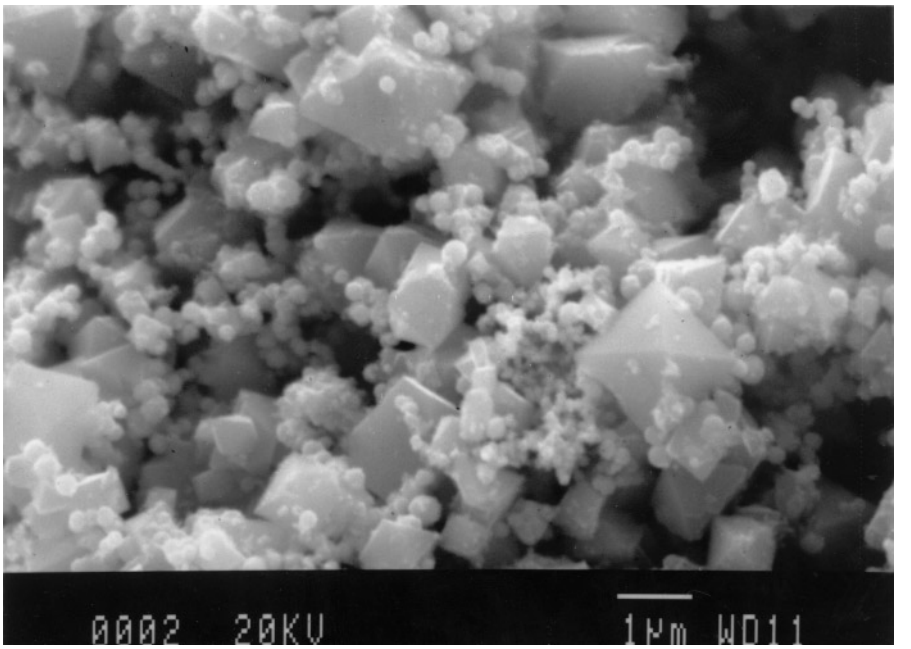

FIG. 6. Scanning electron micrograph showing typical shapes of the particles of the composite in sample A.

2. Microstructure of the Material

The previous samples have been observed by SEM. The powders are made of octahedral particles of various sizes between 0.1 and 2 μm (Fig. 6). The largest of 0.5–2 μm are octahedral, while the smallest are rather round. By imaging with backscattered electrons, the latter are more intense showing that the mean atomic number is higher than in the octahedra. Therefore, the oxide is more concentrated in octahedra than in balls.

The metallic and the spinel phases are easily observed by HRTEM. Both are single crystalline. Figure 7a exhibits two

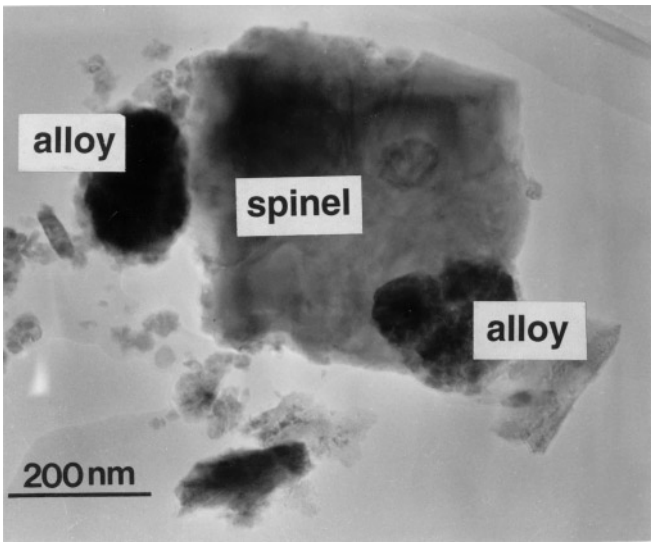

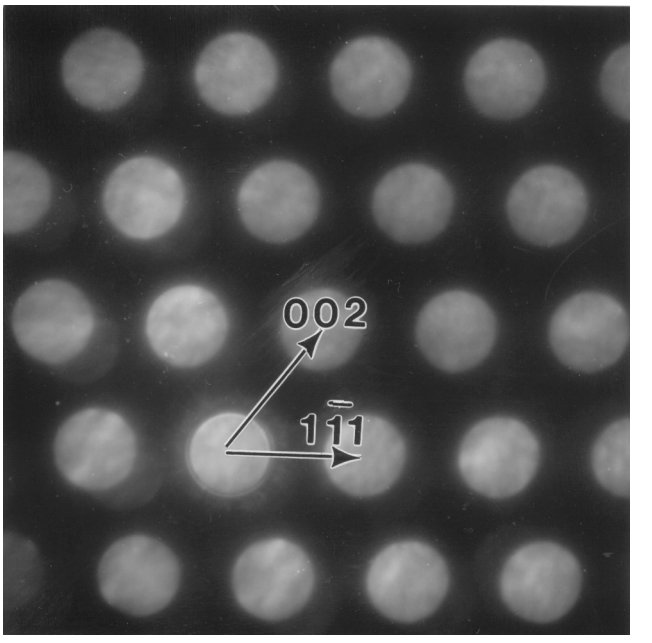

FIG. 7. (a) TEM micrograph showing metallic grains located near a spinel grain. (b) Diffraction pattern of a metallic zone corresponding to the [110] zone axis orientation.

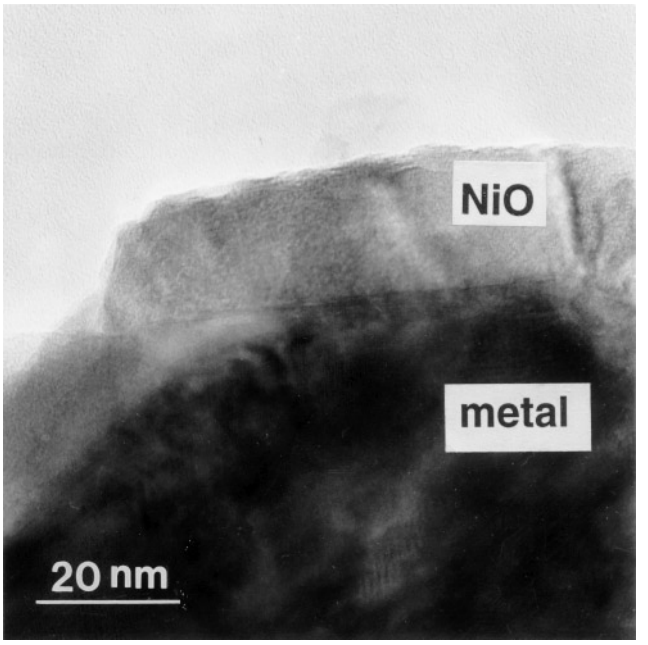

FIG. 8. TEM micrograph of the layer covering the metallic grains. It points out (111) planes of the NiO phase.

metallic grains near the spinel phase observed in the sample Ni/Fe = 0.5. The metallic grains have a ball shape and seem to be not bounded with the spinel ferrite. The diameter of balls is approximatively 150 nm. The diffraction pattern of the metallic zone, corresponding to the (110) zone axis orientation, is characteristic of a single crystal (Fig. 7b). EDSX analyses have been performed at different points of each phase. They show that the metallic phase contains very small amounts of iron and the nickel doped magnetite, low concentration of nickel, in agreement with the previous analysis by XRD. In addition, both phases are heterogeneous. Indeed, the measured Fe/Ni ratios can reach 0.3 at particular points in the metal, while the mean composition determined by XRD corresponds to 0.1. In the spinel phase, the measured Ni/Fe ratios vary between 0.014 and 0.25, the majority of the values being low.

The surface of the metallic grain is presented in Fig. 8. It is covered with a layer of 20 nm made of NiO crystals, itself covered by an amorphous phase 2–3 nm wide. Unfortunately, the layer of amorphous phase is too narrow to be analyzed. The boundary between the metal and NiO is not well defined and is also amorphous.

NiO is also encountered in a thin layer of 10 nm, stuck to well-crystallized large spinel crystal (about 200 nm) and epitaxially related to the spinel phase. Two types of interface between the spinel and NiO are encountered with the following crystallographic relationships:

(i) $\{111\}\langle 101\rangle$ of the spinel is parallel to $\{111\}\langle 101\rangle$ of NiO

(ii) $\{020\}\langle 100\rangle$ of the spinel is parallel to $\{020\}\langle 100\rangle$ of NiO.

These relations are not surprising since both are cubic and their lattice parameters are simply related in a one half ratio ($a_{NiO} = 0.41769$ nm). NiO is itself coated by an amorphous phase 4–5 nm wide, too thin to determine its composition (Fig. 9a). However, this phase crystallizes under the electron beam and the growth of NiO faces occurs along the [111] direction (Fig. 9b). Thus, this amorphous phase may be a nickel hydroxide or hydroxycarbonate.

DISCUSSION

The disproportionation reaction of Fe(II) and the reduction of Ni(II) by Fe^0 leading to an iron–nickel alloy and a spinel phase occurs in a wide range of KOH concentration. Nickel–iron alloy/spinel composites without amorphous phases or hydroxides can be obtained directly in the liquid media for KOH concentrations of at least 14 mol/liter and Ni to Fe ratios lower than 0.2, or after annealing in an argon atmosphere at 800°C.

In the liquid media, Ni(II) is reduced and goes into the metallic phase. Furthermore, nickel is heterogeneously distributed in the spinel phase. As the lattice parameters of Fe_3O_4 and $NiFe_2O_4$ are too far from each other, great quantities of nickel cannot be involved in the spinel phase and the lattice parameter is that of magnetite. Consequently, nickel hydroxide occurs. It forms an amorphous layer, partially dehydrated into NiO, which covers the grains. For Ni to Fe ratios higher than 0.33, it crystallizes. Annealing at 800°C transforms it into NiO which is involved in the oxide phase. Nickel hydroxide has another role. It protects the iron against oxidation by water. Consequently, the metal ratio increases with respect to the oxide when $[Ni]_i/[Fe]_i$ increases.

Metal is in a ball shape. The ball composition is heterogeneous resulting in broad diffraction lines in the X-ray pattern. Furthermore, the metal has a fcc structure and has no crystallographical relationships with the spinel phase, thus, the metal adopts the less energetic shape which is a ball shape. Consequently, there is no direct physical bound between both phases and they can be easily distinguished by SEM. They are just stuck to the spinel phase, while in the Co corresponding composite, the metal is imbricated within the spinel phase and does not exhibit particular shapes (15).

HRTEM and EDXS analyses bring fundamental contributions in the description of the material. First, it demonstrates the compositional heterogeneity of both phases. Iron in metal and nickel in ferrite are not homogeneously distributed. Then, it proves that the metallic balls and the magnetite are covered by NiO and an amorphous layer, which transforms into NiO under the electron beam. Therefore,

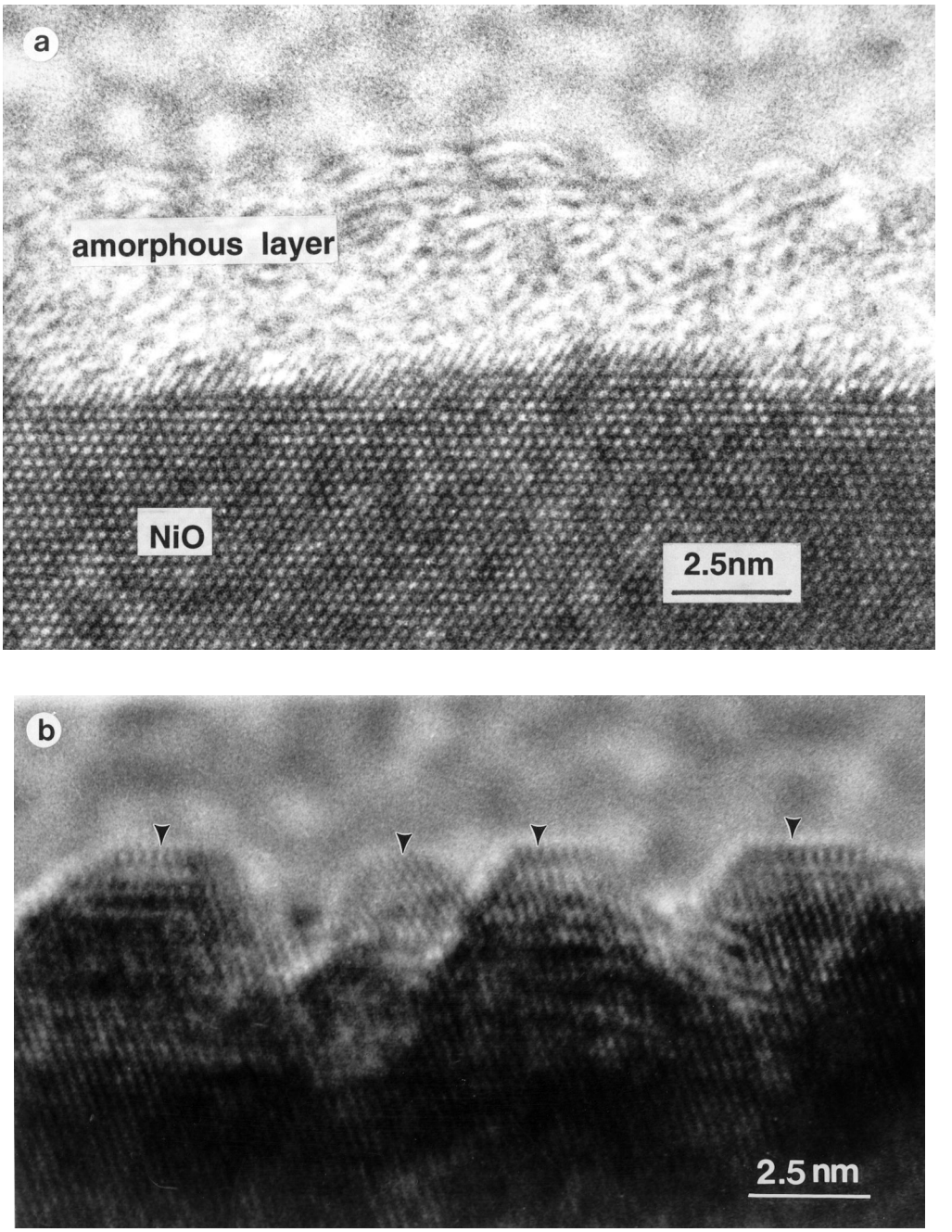

FIG. 9. Development of the coating layer under the electron beam. (a) amorphous layer, (b) NiO produced by the transformation of amorphous phase under the electron beam. Arrows indicate the direction growth of (111) planes.

the metal is passivated and preserved from oxidation by the layer of amorphous and oxide.

REFERENCES

1. R. E. Newnham and S. Trolier-Mc Kinstry, *J. Appl. Cryst.* **23,** 447 (1990).
2. J. J. Mecholsky, *Am. Ceram. Soc. Bull.* **65,** 315 (1986).
3. A. G. Evans, *Mater. Sci. Eng. A* **105–106,** 65 (1988).
4. H. Tamagawa, K. Oyama, T. Yamaguchi, H. Tanaka, H. Tsuiki, and A. Ueno, *J. Chem. Soc. Faraday Trans.* **83,** 3189 (1987).
5. C. Estournes, N. Cornu, and J. L. Guille, *J. Non Cryst. Solids* **170,** 287 (1994).
6. A. Marchand, B. Barbara, P. Mollard, G. Fillion, X. Devaux, and A. Rousset, *J. Magn. Magn. Mat.* **116,** 64 (1992).
7. Ch. Laurent, J. J. Demai, A. Rousset, K. R. Kannan, and C. N. R. Rao, *J. Mater. Res.* **9,** 229 (1994).

8. T. Ambrose, A. Gavrin, and C. L. Chien, *J. Magn. Magn. Mat.* **116,** L311 (1992).
9. P. Matteazi and G. Le Caer, *J. Am. Ceram. Soc.* **75,** 2749 (1992).
10. S. Läkamp, A. Malats I Riera, G. Pourroy, J. L. Dormann, J. M. Greneche, and P. Poix, *Eur. J. Solid State Inorg. Chem.* **32**(2), 159 (1995).
11. A. Malats I Riera, G. Pourroy, and P. Poix, *J. Solid State Chem.* **108,** 362 (1994).
12. A. Malats I Riera, G. Pourroy, and P. Poix, *J. Alloys Compounds* **202,** 113 (1993).
13. S. Läkamp and G. Pourroy, *Eur. J. Solid State Inorg. Chem.* **34,** 295–308 (1997).
14. A. Malats I Riera, G. Pourroy, and P. Poix, *J. Magn. Magn. Mat.* **125,** 125 (1993).
15. J. C. Yamegni-Noubeyo, G. Pourroy, J. Werckmann, A. Malats I Riera, G. Ehret, and P. Poix, *J. Am. Ceram. Soc.* **79,** 2027 (1996).
16. G. Pourroy, S. Ferlay, and J. L. Dormann, *Eur. J. Solid State Inorg. Chem.* **32,** 313 (1995).
17. W. B. Pearson, Handbook of Lattice Spacings and Structures of Metals, Vol. 4, p. 639. Pergamon, Oxford, 1964.